Triassic tectonics of the southern margin of the South China Block

Michel Faure, Wei Lin, Yang Chu, Claude Lepvrier

Triassic tectonics of the Southern margin of the South China Block

Michel Faure[1], Wei Lin[2], Yang Chu[2], Claude Lepvrier[3]

1: Institut des Sciences de la Terre d'Orléans, UMR CNRS Université d'Orléans Campus Géosciences 1A Rue de la Férollerie 45067 Orléans Cedex 2, France

Mail: michel.faure@univ-orleans.fr

2: State Key Laboratory of Lithospheric Evolution, Institute of Geology and Geophysics, Chinese Academy of Sciences, Beijing, China

3: Institut des Sciences de la Terre de Paris, UMR CNRS 7193, Université Pierre & Marie Curie, 75252 Paris Cedex 05 France

ABSTRACT

Middle Triassic orogens are widespread around and inside the South China Block (SCB). The southern peripheral belts that develop from NW to SE, namely Jinshajiang, Ailaoshan, NW Vietnam, NE Vietnam, Yunkai and Hainan exhibit striking similarities, with Permian-Early Triassic magmatic arc, ophiolitic mélange, NE to N-directed synmetamorphic ductile nappes, and fold-and-thrust belt. These collisional belts result from oceanic, then continental subduction of the SCB below Indochina. Eastward of Hainan Island, a Triassic suture is hypothesized offshore of the SCB. Within the SCB, the Xuefengshan is a Middle Triassic intracontinental orogen with NW-directed folds and thrusts, and an intracrustal ductile decollement. This orogen accommodated the Middle Triassic continental subduction of the Western part of the SCB below the Eastern part. At variance to the generally accepted

models, the inter- and intra-continental Triassic orogens of the SCB are interpreted here as the result of South-directed subductions of the SCB.

Key words:
Triassic tectonics, Continental collision, Intracontinental subduction, South China Block, Indochina Block

1. Introduction

It is well acknowledged that the architecture of Asia results of the amalgamation of large continents such as Siberia, N. China, S. China, Tarim, Indochina, India, and several microcontinents: Lhasa, Qiangtang, Qaidam, etc… (e.g. Metcalfe, 2013; Fig. 1). The South China Block (SCB) is one of the most complex as it underwent a long Phanerozoic evolution after its Neoproterozoic formation before 850 Ma during a collisional event that welded the Yangtze and Cathaysia Blocks (e.g. Charvet et al., 1996; Li et al., 2007a; Fig 2). During the Early Paleozoic, the SCB was welded to the N. China block along the Qinling-Dabie belt (e.g. Mattauer et al., 1985; Li et al., 2007b; Faure et al., 2008; Dong et al., 2011; Liu et al., 2013). Between Late Ordovician and Early Silurian, the closure of a Neoproterozoic Nanhua rift was responsible for the building of an intracontinental belt (e.g. Wang and Li, 2003; Faure et al., 2009; Charvet et al., 2010; Wang et al. 2013). From Devonian to Early Triassic, during ca 170 my, the SCB behaved as a stable continent covered by a carbonate platform. However, in the Late Permian, the SW part of SCB, in Yunnan and Guangxi, experienced a huge intraplate magmatism coeval with rifting, known as the Emeishan Large Igneous Province (Ali et al., 2005; Fig. 2).

The Triassic appears as the most important period for the tectonic development of the SCB. Since the recognition of a Norian unconformity and the definition of "Indosinian" movements in Central Vietnam (Deprat, 1915; Fromaget, 1941), the term Indosinian has been ascribed to all Triassic tectonic and magmatic events throughout Asia, even if these features were geodynamically unrelated to Vietnamese ones. As numerous dates are now available, the Middle Triassic stratigraphic age will be preferred to "Indosinian".

Triassic events are widespread all around the SCB (Fig. 2). South of the Early Paleozoic Qinling belt, Triassic top-to-the-S ductile shearing, HP and UHP metamorphism, and plutonism are documented (e.g. Hacker et al., 1998; Lin et al., 2000; Ratschbascher et al. 2003; Li et al. 2007b; Faure et al., 2008; Liu et al., 2013). To the NW, in spite of an intense Cenozoic reworking, a SE-directed Triassic thrusting is recognized in the Longmenshan belt (e.g. Burchfiel et al., 1995; Roger et al. 2008; Robert et al., 2010). The Jinshajiang, Ailaoshan, and N. Vietnam belts represent the Western and Southwestern boundaries of the SCB. Furthermore, Middle Triassic events are responsible for the development of the Xuefengshan belt in the internal part of the SCB (Chu et al., 2012a,b; Wang et al., 2013; Fig. 2). The architecture and geodynamic evolution of these belts are still controversial, but it is widely accepted that the SCB belonged to the upper plate above a north (NE or NW)-dipping subduction zone (e.g. Wang et al., 2013; Li and Li, 2007).

The aim of this paper is to synthesize the Triassic tectonic features that develop along the southern margin of the SCB, and in its interior as well. Then a possible geodynamic interpretation, at variance to the present paradigm, will be discussed. The Triassic events of the northern part of the SCB, and the Jurassic and Cretaceous ones of the interior of SCB will not be addressed here.

2. Triassic orogens of N. Vietnam

It is sometimes proposed that the Red River Fault (RRF) is the boundary between SCB and Indochina. The RRF is a polyphase fault with Miocene sinistral ductile strike-slip (also referred to as the Ailaoshan-Red River shear zone), and a Plio-Quaternary dextral motion. The left-lateral ductile displacement developed in response to the Indian collision was variously estimated from a few tens to several hundred of km (e.g. Tapponnier et al., 1986; Leloup et al., 1995, 2006; Searle, 2006). The strike-slip faulting accounts for the Cenozoic tectonics, but when dealing with the Triassic events, the RRF cannot be considered as a plate boundary as ophiolites, subduction complexes, or HP metamorphic rocks are lacking. In contrast, two ophiolitic belts are recognized in NW and NE Vietnam on both sides of the RRF, along the Song Chay and Song Ma faults (Fig. 2; Lepvrier et al., 1997, 2008, 2011; Faure et al., 2014).

2.1. The NW Vietnam (Song Ma) belt

From SW to NE, several litho-tectonic zones are recognized (Figs. 2, 3A). 1) Permian-Early Triassic volcanic and sedimentary rocks of the *Sam Nua zone*, overlying an Early Paleozoic series, are interpreted as a magmatic arc (Tran et al., 2008a; Liu et al., 2012). 2) The *Song Ma zone* formed by ultramafic, mafic rocks and deep marine sediments represents an ophiolitic suture. 3) The *Nam Co metamophic rocks*, developed at the expense of Neoproterozoic terrigenous series, and Paleozoic limestone and sandstone, correspond to the sedimentary cover of a continental basement ductilely deformed during the NE-ward thrusting of the Song Ma ophiolites. 4) Farther North, folded unmetamorphosed successions of Devonian to Carboniferous limestone, Permian volcanics, Early Triassic clastics, and Middle Triassic carbonates represent the outer zone (*Son La-Lai Chau zone*) of this belt. There, Late Permian alkaline basalts and volcaniclastites form the Song Da rift. Although sometimes considered as ophiolites, these rocks, emplaced in an intraplate setting, belong to

99 the Emeishan Large Igneous Province (Ali et al., 2005; Tran et al., 2008b; Tran and Vu,
100 2011). The Permian Tule acidic rocks are also relevant to this bimodal magmatism (Tran and
101 Vu, 2011). 5) Lastly, the Proterozoic basement, stratigraphically overlain by a Paleozoic
102 sedimentary cover, is called the *Posen-Hoabinh zone* that forms the deepest part of the NW
103 Vietnam belt.

104 The NW Vietnam belt exhibits a structural and metamorphic polarity decreasing from
105 SW to NE. Late Triassic sandstone and conglomerate unconformably cover deformed rocks.
106 Biotite and muscovite $^{40}Ar/^{39}Ar$, zircon U/Pb, and monazite chemical U/Th/Pb ages around
107 245-230 Ma argue for a Middle Triassic age for the nappe architecture of the NW Vietnam
108 belt (Lepvrier et al., 1997, 2008, Nakano et al., 2008, 2011).
109
110 *2.2. The NE Vietnam (Song Chay) belt*

111 NE of the RRF, another Triassic belt develops with the following SW to NE zonation
112 (Lepvrier et al. 2011; Faure et al. 2014; Figs. 2, 3A). 1) The *Dai Nuy Con Voi* is a NW-SE
113 striking Cenozoic HT antiform developed from grauwacke and pelite hosting granodiorite,
114 diorite and gabbro plutons of Permian-Triassic age (Gilley et al., 2003; Zelazniewicz et al.
115 2013). This zone is interpreted as a magmatic arc. 2) The *Song Chay ophiolitic mélange* is
116 composed of serpentinites, mafic rocks, limestone, and chert blocks included in a terrigenous
117 matrix of Triassic age. 3) The *NE Vietnam nappe* consists of Cambrian-Ordovician
118 terrigenous rocks, and Devonian to Permian carbonates. Ordovician porphyritic granites (e.g.
119 the Song Chay massif) are now changed into augengneiss. N- to NE-verging folds and thrusts
120 deform the entire lithological succession. Biotite-garnet-staurolite micaschist yields a
121 monazite U-Th-Pb age at 246±10 Ma (Faure et al., 2014). 4) The *outer zone* is a Paleozoic
122 lithological succession similar to that of the NE Vietnam nappe covered by a thick Middle
123 Triassic turbidite series with acidic lava flows and ashes. This formation includes olistoliths

of alkaline basalt, gabbro and limestone. Similar mafic rocks crop out in China where they intrude the late Paleozoic limestone platform. They have been ascribed to the "Babu ophiolites" (Fig. 2, Zhong 2000; Cai and Zhang, 2009), but their geological setting and geochemistry show that they are intraplate basalts corresponding to remote parts of the Emeishan Large Igneous Province (e.g. Zhou et al. 2006, see discussion in Faure et al., 2014). The NE Vietnam belt extends in China between Kunming and Nanning, the flat lying Late Paleozoic limestone platform is involved in N-directed folds and thrusts upon the Middle Triassic turbidite (Fig. 4C).

In summary, both the NW and SE Vietnam belts are collisional orogens formed by a SW-ward subduction of oceanic, then continental lithosphere. Due to their lithological, structural, and chronological similarities, the two belts have been interpreted as the result of a duplication of a single Triassic orogen by the Cenozoic left-lateral strike-slip shearing of the Ailaoshan-Red River shear zone (Faure et al., 2014).

3. The western extension of the N. Vietnam orogens

3.1. The Ailaoshan Belt

This NW-SE 500km-long belt (Fig. 2) is subdivided into several narrow stripes by belt-parallel strike-slip faults. In spite of the intense Cenozoic shearing (e.g. Leloup et al., 1995), the Ailaoshan is commonly acknowledged as a Triassic suture zone between the SCB and Indochina-Simao block but structural details and subduction polarity are disputed (e.g. Zhong 2000; Jian et al., 2009a,b; Fan et al., 2010; Lai et al., 2013a,b; Wang et al., 2013). From SW to NE, four litho-tectonic zones ascribed to the Triassic orogen are recognized (Fig. 2). 1) The *Western Ailaoshan*, characterized by volcanic and sedimentary rocks, is unconformably overlain by Late Triassic red conglomerate and sandstone. Basalt and andesite, dated between 287 and 265 Ma, were originated in a magmatic arc installed upon a

149 Silurian-Devonian terrigenous series (Jian et al., 2009a; Fan et al., 2010). 2) The *Central*
150 *Ailaoshan* contains serpentinite, gabbro, dolerite, plagiogranite, basalt, chert, and limestone
151 blocks enclosed into a terrigenous matrix (Lai et al., 2014b). Zircon from plagiogranite yields
152 U-Pb ages at 383-376 Ma, 365 Ma, and 328 Ma interpreted crystallization age of ophiolitic
153 protoliths (Jian et al., 2009b; Lai et al., 2014b). This domain represents an ophiolitic mélange
154 but the age of the matrix is unknown. 3) The *Eastern Ailaoshan* consists of gneiss, micachists,
155 amphibolites, marbles, and migmatites that form a Paleoproterozoic basement, partly
156 reworked during the Cenozoic (Lin et al., 2012). Middle Triassic carbonate covers the
157 crystalline basement. 4) The *Jinping area* exposes Late Permian mafic lava, pillow breccia,
158 agglomerate, and volcaniclastites (Wang et al., 2007). Furthermore, felsic volcanites dated at
159 ca 246 Ma result of syn- to late-collisional crustal melting (Lai et al., 2014a).
160 A steeply dipping foliation and a subhorizontal lineation are the main ductile
161 structures developed during the Cenozoic shearing as they involve the Late Triassic rocks.
162 Nevertheless, a steeply dipping stretching lineation with top-to-the NE sense of shear and NE
163 verging folds are also observed (Fig 4B). These structures, incompatible with the strike-slip
164 event, and not observed in the Late Triassic or younger rocks, are of Middle Triassic in age.
165 Thus in spite of the Tertiary overprint, the Ailaoshan belt is comparable with the N.
166 Vietnam belts. Namely, the Western, Central, and Eastern Ailaoshan zones are equivalent to
167 the Sam Nua, Song Ma, Posen-Hoabinh zones, respectively. The Sonla-Laichau zone pinches
168 out in the Ailaoshan, except in the Jinping area where magmatic rocks are similar to the Song
169 Da rift.
170
171 *3.2. The termination of the NE Vietnam Belt*
172 The NE Vietnam Belt abruptly ends in China (Fig. 2). The Dai Nuy Con Voi
173 metamorphics are surrounded by Permian-Early Triassic volcanites and grauwackes

corresponding to the magmatic arc, but ophiolites are not exposed. Folded and thrusted Paleozoic rocks are equivalent to the NE Vietnam nappe. To the north, Middle Triassic turbidites of the Youjiang basin involved in N-verging folds correlate with the outer zone of NE Vietnam.

3.3. The Jinshajiang Belt

At the edge of the Tibet plateau, the Triassic Jinshajiang orogen is documented by the Late Triassic unconformity overlying a folded Middle Triassic ophiolitic mélange with basalt, chert, and limestone blocks (Fig. 4A, Zhong 2000; Wang and Metcalfe, 2000). This mélange overthrusts to the East the Late Paleozoic-Triassic carbonate platform of the SCB. To the West, a Permian-Early Triassic magmatic arc argues for a west-directed subduction. The bimodal magmatism at 245-237 Ma is interpreted as syn- to post-collisional (Zi et al., 2012). The Jianshajiang Belt exhibits lithological and structural features similar to those of the Ailaoshan and N Vietnam orogens.

4. The eastern extension of the N. Vietnam orogens

4.1. The Yunkai Massif

In Guangxi, the Late Triassic-Jurassic red sandstone of the Shiwandashan basin (SB in Fig. 2) is a post-orogenic molasse with respect to the Triassic orogeny (e.g. Hu et al., 2014). The Yunkai massif consists of Early Paleozoic HT metamorphics, migmatites, and Triassic granites tectonically surrounded by weakly metamorphosed Devonian-Carboniferous sedimentary rocks (e.g. Wang et al., 2007; Lin et al., 2008). The metamorphic rocks belong to the Early Paleozoic orogen of SE China but were intensely reworked by the Triassic events. The flat-lying foliation and NE-SW stretching lineation, associated with a top-to-the-NE ductile shearing developed at ca 250-240 Ma. During this event, the Early Paleozoic granites

were changed to orthogneiss (Fig. 4D). The Yunkai massif is a 100km-scale basement nappe that overthrusts northward onto the Late Paleozoic sedimentary rocks of the SCB (Figs. 3C, 4E). As ophiolites are lacking there, the eastward extension of the Song Chay suture should be searched more to the South in Hainan Island (Fig.2).

4.2. Triassic tectonics in Hainan Island

The tectonic evolution of Hainan Island remains controversial. The Cretaceous and younger extensional events are not considered here. Late Triassic plutons seal the main ductile deformation (Fig. 3B). N-verging folds and thrusts deform the Early Paleozoic series and the underlying Proterozoic basement. Granodiorites and biotite granite with calcalkaline geochemical signatures, and yielding zircons SHRIMP U-Pb ages at 267±3Ma Ma and 263±3 Ma by SHRIMP method, are interpreted as the "Wuzishan magmatic arc" (Li et al., 2006). North of this arc, a Late Permian-Early Triassic terrigenous series including Carboniferous gabbro, basalt, siliceous rocks and limestone is interpreted as a mélange (Fig. 4F; Li et al., 2002). This formation is ductilely deformed with top-to-the-N kinematics dated at ca 250-240 Ma by $^{40}Ar/^{39}Ar$ method on micas (Zhang et al., 2011). In spite of a still limited knowledge, the Hainan Island appears as a suitable site for the eastern extension of the Song Chay suture.

5. Triassic intracontinental tectonics in East SCB

5.1. The Xuefengshan Belt

Middle Triassic tectonics is not limited to the SCB margins. In central SCB (E. Hunan and Guangxi), the Xuefengshan Belt is a NNE-SSW striking 700 km long belt dominated by NW-directed thrusts and folds. SE-verging folds are interpreted as secondary back-folds (Chu et al., 2012a; Fig. 5). A ductile decollement layer, intruded by Late Triassic plutons dated at 225-215 Ma by SIMS U-Pb method on zircon (Chu et al., 2012c), exhibits a NW-SE striking

stretching lineation, and top-to-the-NW sense of shear (Chu et al., 2012b). This 500 km wide fold-and-thrust belt involves the entire Neoproterozoic to Early Triassic sedimentary pile to the west of the Chenzhou-Linwu fault (CLF in fig. 2). This fault, devoid of ophiolites and subduction mélange, is not a suture zone, but an intracontinental "scar". In order to balance the ca 300 km of shortening experienced by the sedimentary rocks overlying the decollement layer, a SE-ward continental subduction of the same amount must have taken place in the crystalline basement of the western part of SCB (Chu et al., 2012a).

5.2. Coastal and eastern SE China

E-W striking folds develop south of the Jiangshan-Shaoxing Fault (Fig. 2). The Late Triassic regional unconformity argues for a Middle Triassic event (Shu et al., 2008). As documented in the Jiuling area (Chu and Lin, 2014), upright folds are lateral ramps related to the Xuefengshan belt. The E-W elongated Wugongshan dome located immediately south of the Jiangshan-Shaoxing fault (Fig. 2; Faure et al., 1996) might be also developed during the reactivation of this Neoproterozoic suture. The Triassic ductile deformation is probably underestimated in the eastern part of SCB (Wang et al. 2014).

In the coastal area of SE China, widespread Jurassic and Cretaceous granites and volcanites hide older formations. West of Fuzhou, Middle Triassic rocks deformed by N-verging recumbent folds and covered by a Late Triassic unconformity indicate that the SE China coastal area also experienced a Middle Triassic deformation (Zhu et al., 1996).

6. Discussion of the Triassic orogens

A N-directed Triassic oceanic subduction, below the SCB, is often suggested (e.g. Zhou and Li, 2000; Li and Li, 2007). This view is based on the assumption that the active continental margin of SCB existed since the Middle Permian (Li et al., 2006, 2012). Indeed,

249 an active margin setting has been documented for the Cretaceous, but the geochemistry of the
250 Jurassic magmatism supports rather an intraplate setting (Chen et al., 2008). As in Vietnam, in
251 Hainan, the relative positions of the mélange and arc argue for a South-directed subduction. In
252 SE China, most of the Late Triassic plutons are S-type due to the melting of Proterozoic
253 sediments, and a small amount of A-type plutons also exists (e.g. Li et al., 2006; Chen et al.,
254 2011; Sun et al., 2011; Zhao et al., 2012; Wang et al. 2013). The tectonic setting of these
255 plutons is not documented. Furthermore, their emplacement ages do not clearly show a NW-
256 to-SE polarity that might be related to a N-directed subduction.
257 Therefore, an alternative interpretation is tentatively proposed here. The NW-directed
258 shearing and 300 km shortening recorded by the sedimentary series of the Xuefengshan Belt
259 are balanced by the same amount of continental subduction. This means that during the
260 Triassic, the SE China lithosphere was underlain by a slab corresponding to the SE-ward
261 subducted lithosphere of the Western part of SCB (Figs. 6,7).
262 Along the SE China coast, evidence for a Triassic subduction is not documented.
263 Assuming an eastward extension of the Jinshajiang-Ailaoshan-N Vietnam-Hainan belt would
264 imply that the SCB represents the lower plate. Such a polarity may account for the thrusting
265 sense observed in Yunkai, Hainan, and SE China. The Triassic peraluminous plutons (e.g.
266 Darongshan granite, DS in Fig. 2) emplaced in the footwall of the major thrust zones during
267 deep-seated thrusting coeval with melting. Moreover, Permian arc magmatism is documented
268 in Mindoro Island of W. Philippines (Fig. 1; Knittel et al., 2010). Considering the Cenozoic
269 opening of the S. China sea, this arc represents the eastern extension of the Wuzishan arc of
270 Hainan. Triassic ophiolites and tectonics are unknown in the Philippines, but the Tailuko belt
271 of Taiwan that exposes the deepest rocks of the island yields garnet-chloritoid-kyanite-
272 staurolite micaschist with metamorphic zircon dated at 200±22 Ma (Yui et et al., 2009; Fig.
273 2). Furthermore, HP metamorphic rocks crop out in the S. Ryukyu Islands (Fig.2). In these

mafic schists, phengite and barroisite are dated at 225±5 Ma and 237±6 Ma Ma, respectively (Faure et al., 1988). One possibility is to relate these features to the Triassic orogeny of SCB.

In conclusion, the Triassic belts that wrap around the SCB southern margin from SW to SE exhibit lithostratigraphic, structural and chronological resemblances that allow us to infer that a single belt developed in response to the subduction and collision of the SCB below the Qiangtang-Indochina block. Such a S-directed subduction was coeval with the intra-continental subduction responsible for the development of the structures in SE China. Work in progress aims at testing this new interpretation.

Acknowledgements

The authors are grateful to I. Manighetti and B. Mercier de Lépinay for their invitation to pay a tribute to J-F Stéphan who devoted his scientific activity to the understanding of orogenic processes, and particularly to the geodynamics of SE Asia. The constructive comments of H. Leloup, B. Mercier de Lépinay and I. Manighetti are acknowledged. This work has been supported by NSFC grants 41225009 and 41472193 and a Major State Special Research on Petroleum project 2011ZX05008-001.

References

Ali, J., Thompson, G.M., Zhou, M.-F., Song, X., 2005. Emeishan large igneous province, SW China. Lithos 79, 475–499.

Burchfiel, B.C., Chen, Z., Liu, Y., Royden, L.H., 1995. Tectonic of the Longmen Shan and adjacent regions. International Geology Review 37, 661–735.

299 Cai, X., Zhang, K.J., 2009. A new model for the Indochina and South China collision
300 during the Late Permian to the Middle Triassic. Tectonophysics 467, 35–43.
301
302 Charvet, J., Shu, L.S., Shi, Y.S., Guo, L.Z., Faure, M., 1996. The building of South China:
303 collision of Yangtzi and Cathaysia blocks, problems and tentative answers. J. Southeast Asian
304 Earth Sciences 13, 223–235.
305
306 Charvet, J., Shu, L.S., Faure, M., Choulet, F., Wang, B., Le Breton, N., 2010. Structural
307 development of the Lower Paleozoic belt of South China: genesis of an intracontinental
308 orogen. J. Asian Earth Sci. 39, 309–330.
309
310 Chen, C.H., Lee, C.Y., Sinjo, R., 2008. Was there Jurassic paleo-Pacific subduction in south
311 China? Constraints from 40Ar/39Ar dating, elemental and Sr-Nd-Pb isotopic geochemistry of
312 the Mesozoic basalts. Lithos 106, 83-92.
313
314 Chen, C.H., Hsieh, P.S., Lee, C.Y., Zhou, H.W., 2011. Two episodes of the Indosinian
315 thermal event on the South China Block: constraints from LA-ICPMS U–Pb zircon and
316 electron microprobe monazite ages of the Darongshan S-type granitic suite. Gondwana
317 Res. 19, 1008–1023.
318
319 Chu, Y., Faure, M. Lin, W. Wang, Q. 2012a. Early Mesozoic tectonics of the South China
320 block: Insights from the Xuefengshan intracontinental orogen, J. Asian Earth Sci. 61, 199–
321 220.
322
323 Chu, Y., Faure, M., Lin, W., Wang, Q., Ji, W., 2012b. Tectonics of the Middle Triassic

intracontinental Xuefengshan Belt, South China: new insights from structural and chronological constraints on the basal decollement zone. International J. Earth Sci. 101, 2125–2150.

Chu, Y., Lin, W., Faure, M., Wang, Q., Ji, W., 2012c. Phanerozoic tectonothermal events of the Xuefengshan Belt, central South China: implications from U-Pb age and Lu-Hf determinations of granites. Lithos 150, 243–255.

Chu, Y., Lin, W., 2014. Phanerozoic polyorogenic deformation in southern Jiuling Massif, northern South China block: Constraints from structural analysis and geochronology. J. Asian Earth Sci. 86, 117–130.

Deprat, J., 1915. Etudes géologiques sur la région septentrionale du Haut-Tonkin. Mémoire du Service Géologique de l'Indochine, Hanoi IV, 174pp.

Dong, Y., Zhang, G., Neubauer, F., Liu, X., Genser, J., Hauzenberger, C., 2011. Tectonic evolution of the Qinling orogen, China: Review and synthesis. J. Asian Earth Sci. 41, 213–237.

Fan, W.M., Wang, Y.J., Zhang, A.M., Zhang, F.F., Zhang, Y.Z., 2010. Permian arc–back-arc basin development along the Ailaoshan tectonic zone: geochemical, isotopic and geochronological evidence from the Mojiang volcanic rocks, Southwest China. Lithos 119, 553–568.

348 Faure, M., Monié, P., Fabbri, O., 1988. Microtectonics and $^{40}Ar/^{39}Ar$ dating of high pressure
349 metamorphic rocks of the South Ryukyu arc, and their bearings on the pre-Eocene
350 geodynamic evolution of E. Asia. Tectonophysics 56, 133-143.
351
352 Faure, M., Sun, Y., Shu, L., Monié, P. , Charvet, J., 1996. Extensional tectonics within a
353 subduction-type orogen. The case study of the Wugongshan dome (Jiangxi Province, SE
354 China). Tectonophysics, 263, 77-108.
355
356 Faure, M., Lin, W., Schärer, U., Shu, L., Sun, Y., Arnaud, N., 2003. Continental subduction
357 and exhumation of UHP rocks. Structural and geochronological insights from the Dabieshan
358 (E. China), Lithos 70, 213–241.
359
360 Faure, M., Lin, W., Monié, P., Meffre, S., 2008. Palaeozoic collision between the North and
361 South China blocks, Triassic intracontinental tectonics, and the problem of the ultrahigh-
362 pressure metamorphism. C. R. Geoscience 340, 139–150.
363
364 Faure, M., Shu, L.S., Wang, B., Charvet, J., Choulet, F., Monié, P., 2009. Intracontinental
365 subduction: a possible mechanism for the Early Paleozoic Orogen of SE China. Terra Nova
366 21, 360–368.
367
368 Faure, M., Lepvrier, C., Nguyen, V.V., Vu, V.T., Lin, W. Chen, Z. 2014. The South China
369 block-Indochina collision: Where, when, and how? J. Asian Earth Sci. 79, 260–274.
370

371 Fromaget, J., 1941. L'Indochine française, sa structure géologique, ses roches, ses mines et
372 leurs relations possibles avec la tectonique. Bulletin du Service Géologique de l'Indochine 26,
373 1–140.
374
375 Gilley, L.D., Harrison, T.M., Leloup, P.H., Ryerson, F.J., Lovera, O.M., Wang, J.H., 2003.
376 Direct dating of left-lateral deformation along the Red River shear zone, China, Vietnam. J.
377 Geophysical Res. 108. http://dx.doi.org/10.1029/ 2001JB0011726.
378
379 Hacker, B., Ratsbascher, L., Webb, L., Ireland, T.,Walker, D., Suwen, D. 1998. U/Pb zircon
380 ages constrain the architecture of the ultrahigh-pressure Qinling–Dabie orogen, China, Earth
381 Planet. Sci. Lett. 161, 215–230.
382
383 Hu, L., Du Y. Cawood, P., Xua, Y., Yua, W., Zhua, Y., Yang, J. 2014. Drivers for late
384 Paleozoic to early Mesozoic orogenesis in South China: Constraints from the sedimentary
385 record. Tectonophysics 618, 107–120
386
387 Jian, P., Liu, D.Y., Kroener, A., Zhang, Q., Wang, Y.Z., Sun, X.M., Zhang, W., 2009a.
388 Devonian to Permian plate tectonic cycle of the Paleo-Tethys Orogen in Southwest
389 China (I): geochemistry of ophiolites, arc/back-arc assemblages and within plate
390 igneous rocks. Lithos 113, 748–766.
391
392 Jian, P., Liu, D.Y., Kroener, A., Zhang, Q., Wang, Y.Z., Sun, X.M., Zhang, W., 2009b.
393 Devonian to Permian plate tectonic cycle of the Paleo-Tethys orogen in Southwest China
394 (II): insights from zircon ages of ophiolites, arc/back-arc assemblages and within plate
395 igneous rocks and generation of the Emeishan CFB Province. Lithos 113, 767–784.

Knittel, U., Hung, C.-H., Yang, T.F., Iizuka, Y., 2010. Permian arc magmatism in Mindoro, the Philippines: an early Indosinian event in the Palawan Continental Terrane. Tectonophysics 493, 113–117.

Lai, C.K, Meffre, S., Crawford, A., Zaw, K., Xue, C.D., Halpin, J. 2014a. The Western Ailaoshan Volcanic Belts and their SE Asia connection: A new tectonic model for the Eastern Indochina Block. Gondwana Res. 26, 52-74.

Lai, C.K., Meffre, S. Crawford, A., Khin Zaw, K., Halpin, J., Chuan-Dong Xue, C.D., Salam, A. 2014b. The Central Ailaoshan ophiolite and modern analogs. Gondwana Res. 26, 75-88.

Leloup, H., Lacassin, R., Tapponnier, P., Schärer, U., Zhong, D., Liu, X., Zhang, L., Ji, S., Trinh, P., 1995. The Ailaoshan-Red River shear zone (Yunnan, China), Tertiary transform boundary of Indochina. Tectonophysics 252, 3–84.

Leloup, H., Tapponnier, P., Lacassin, R., 2006. Discussion on the role of the Red River shear zone, Yunnan and Vietnam, in the continental extrusion of SE Asia. J. Geological Society, London, 164, 1253-1260.

Lepvrier, C., Maluski, H., Van Vuong, Nguyen., Roques, D., Axente, V., Rangin, C., 1997. Indosinian NW-trending shear zones within the Truong Son belt (Vietnam): ^{40}Ar-^{39}Ar Triassic ages and Cretaceous to Cenozoic overprints. Tectonophysics 283, 105–127.

420 Lepvrier, C., Nguyen, V.V., Maluski, H. Truong, T.P., Vu.V. T., 2008. Indosinian tectonics in
421 Vietnam. C. R. Geoscience 340, 94–111.
422
423 Lepvrier, C., Faure, M., Nguyen, V. V., Vu, V.T., Lin, W., Thang, T.T., Phuong, H. 2011.
424 North-directed Triassic nappes in Northeastern Vietnam (East Bac Bo). J. Asian Earth Sci. 41,
425 56–68.
426
427 Li, XH., Zhou, H., Chung, SL., Ding, S., Liu, Y., Lee, C.Y., Ge, W., Zhang, Y., Zhang, R.,
428 2002. Geochemical and Sm-Nd isotopic characteristics of metabasites from central Hainan
429 Island, South China and their tectonic significance. The Island Arc, 11, 193-205.
430
431 Li, XH., Li, ZX., Li, WY., Wang, Y. 2006. Initiation of the Indosinian orogeny in South
432 China: Evidence for a Permian magmatic arc on Hainan Island. J. Geology, 114, 341-353.
433
434 Li, ZX., Li, XH. 2007. Formation of the 1300 km-wide intracontinental orogen and post-
435 orogenic magmatic province in Mesozoic South China: a flat-slab subduction model. Geology
436 35, 179-182.
437
438 Li, ZX., Wartho, J.A., Occhipinti, S. Zhang, C.L., Li, X.H., Wang, J., Bao, C.M. 2007a. Early
439 history of the eastern Sibao orogenic belt (South China) during the assembly of Rodinia: new
440 mica $^{40}Ar/^{39}Ar$ dating and SHRIMP U-Pb detrital zircon provenance constraints. Precambrian
441 Res. 159, 79-94.
442

443 Li, S.Z., Kusky, T.M., Wang, L., Zhang, G.W., Lai, S.C., Liu, X.C., Dong, S.W., Zhao, G.C.,
444 2007b. Collision leading to multiple-stage large-scale extrusion in the Qinling orogen:
445 Insights from the Mianlue suture. Gondwana Res. 12, 121–143.
446
447 Li XH., Li, ZC., He, B., Li, WC., Li, QL., Gao, Y., Wang, XC., 2012. The Early Permian
448 active continental margin and crustal growth of the Cathaysia Block: In situ U–Pb, Lu–Hf and
449 O isotope analyses of detrital zircons. Chem. Geol. 328, 195–207.
450
451 Lin, W., Faure, M., Monié, P., Schäerer, U., Zhang, L., Sun, Y., 2000. Tectonics of SE China,
452 new insights from the Lushan massif (Jiangxi Province), Tectonics 19, 852–871.
453
454 Lin, W., Wang, QC., Chen, K., 2007. Phanerozoic tectonics of south China block: new
455 insights from the polyphase deformation in the Yunkai massif. Tectonics 27, 1-16.
456
457 Lin, T.H., Chung, S.L., Chiu, H.Y., Wu, F.Y., Yeh, M.W., Searle, M., Iizuka, Y., 2012.
458 Zircon U-Pb and Hf isotope constraints for the Ailaoshan-Red River shear zone on the
459 tectonic and crustal evolution of southwestern China. Chem. Geol. 291, 23-27.
460
461 Liu, JL. Tran, M., Tang, Y., Nguyen, Q.L., Tran, T.H. , Wu, W., Chen, J., Zhang, Z., Zhao,
462 Z., 2012. Permo-Triassic granitoids in the northern part of the Truong Son belt, NW Vietnam:
463 geochronology, geochemistry and tectonic implications. Gondwana Res. 122, 628–644.
464
465 Liu X., Jahn, B-M., Li, S., Liu, Y., 2013. U-Pb zircon age and geochemical constraints on
466 tectonic evolution of the Paleozoic accretionary orogenic system in the Tongbai orogen,
467 central China. Tectonophysics 599, 67–88.

Mattauer, M., Matte, P., Malavieille, J., Tapponnier, P., Maluski, H., Z. Xu, Z., Y. Lu, Y., Tang, Y., 1985. Tectonics of the Qinling Belt: buildup and evolution of eastern Asia, Nature 317, 496–500.

Metcalfe, I. 2013. Gondwana dispersion and Asian accretion: tectonic and palaeogeographic evolution of eastern Tethys. J. Asian Earth Sciences 66, 1–33.

Nakano, N., Osanai, Y., Nguyen, T.M., Miyamoto, T., Hayasaka, Y., Owada, M., 2008. Discovery of high-pressure granulite-facies metamorphism in northern Vietnam: constraints on the Permo-Triassic Indochinese continental collision. C. R. Geosciences 340, 127–138.

Nakano, N., Osanai, Y., Sajeev, K., Hayasaka, Y., Miyamoto, T., Minh, Nguyen Thi, Owada, M., 2010. Triassic eclogite from northern Vietnam: inferences and geological significance. J. Metamorphic Geology 28, 59–76.

Ratschbacher, L., Hacker, B., Calvert, A. Webb, L., Grimmer, J., Mc Williams, M., Ireland, T., Dong, S., Hu, J., 2003. Tectonics of the Qinling (Central China): tectonostratigraphy, geochronology, and deformation history, Tectonophysics 366, 1–53.

Robert, A., Pubellier, M., de Sigoyer, J., Vergne, J., Lahfid, A., Cattin, R., Findling, N., Zhu, J., 2010. Structural and thermal characters of the Longmenshan (Sichuan, China). Tectonophysics 491, 165-173.

492 Roger, F., Jolivet, M., Malavieille, J., 2008. Tectonic evolution of the Triassic fold belts of
493 Tibet. C. R. Geoscience 340, 180-189.
494
495 Searle, M.P., 2006. Role of the Red River shear zone, Yunnan and Vietnam, in the
496 continental extrusion of SE Asia. J. Geological Society 163, 1025–1036.
497
498 Shu, L.S., Faure, M., Wang, B., Zhou, X.M., Song, B., 2008. Late Palaeozoic–Early
499 Mesozoic geological features of South China: Response to the Indosinian collision events in
500 Southeast Asia. C.R. Geoscience 340, 151–165.
501
502 Sun, Y., Ma, C.-Q., Liu, Y.-Y., She, Z.-B., 2011. Geochronological and geochemical
503 constraints on the petrogenesis of Late Triassic aluminous A-type granites in southeast
504 China. J. Asian Earth Sci. 42, 1117–1131.
505
506 Tapponnier, P., Lacassin, R., Leloup, H., Schärer, U., Zhong, D., Liu, X., Ji, S., Zhang, L.,
507 Zhong, J., 1990. The Ailaoshan-Red river metamorphic belt: tertiary left-lateral shear between
508 Indochina and South China. Nature 343, 431–437.
509
510 Tran, T.H., Tran, T.A., Ngo, T.P., Pham, T.D., Tran, V.A., Izokh, A., Borisenko, A.,
511 Lan, C.Y., Chung, S.L., Lo, C.H., 2008a. Permo-Triassic intermediate-felsic magmatism of
512 the Truong Son belt, eastern margin of Indochina. C. R. Geoscience 340, 112–126.
513
514 Tran, T.H., Izokh, A.E., Polyakov, G.V., Borisenko, A.S., Tran, T.A., Balykin, P.A., Ngo,
515 T.P., Rudnev, S.N., Vu, V.V., Bui, A.N., 2008b. Permo-Triassic magmatism and metallogeny

516 of Northern Vietnam in relation to the Emeishan plume. Russian Geology and Geophysics 49,
517 480–491.
518
519 Tran, VT., Vu, K., (Eds.), 2011. Geology and Earth Resources of Vietnam, General Dept of
520 Geology, and Minerals of Vietnam, Hanoi, Publishing House for Science and Technology,
521 634 pp.
522
523 Wang, J., Li, Z.X., 2003. History of Neoproterozoic rift basins in South China: implications
524 for Rodinia break-up. Precambrian Res. 122, 141–158.
525
526 Wang, X., Metcalfe, I. Jiang, P., He, L., Wang, C., 2000. The Jinshajiang-Ailaoshan suture
527 zone: tectonostratigraphy, age and evolution. J. Asian Earth Sci. 18, 675–690.
528
529 Wang, C., Zhou, MF, Qi, L., 2007. Permian flood basalts and mafic intrusions in the
530 Jinping (SW China)-Song Da (northern Vietnam) district: mantle sources, crustal
531 contamination and sulfide segregation. Chem. Geol. 243, 317–343
532
533 Wang, YJ., Fan, W., Cawood, P., Ji, S., Peng, T., Chen, X., 2007. Indosinian high-strain
534 deformation for the Yunkaidashan tectonic belt, south China: kinematics and $^{40}Ar/^{39}Ar$
535 geochronological constraints. Tectonics 26, 1-21.
536
537 Wang, YJ., Fan, W., Zhang, G., Zhang, Y. 2013. Phanerozoic tectonics of the South China
538 Block: Key observations and controversies. Gondwana Res. 23, 1273–1305.
539

Wang, B., Shu, L.S., Faure, M., Jahn, B-M., Lo, C-H., Charvet, J., Liu, H., 2014. Phanerozoic multistage tectonic rejuvenation of the continental crust of the Cathaysia Block: Insights from structural investigations and combined zircon U-Pb and mica $^{40}Ar/^{39}Ar$ geochronology of the granitoids in Southern Jiangxi province. J. Geology 122, 309–328.

Yu, T.F., Okamoto, K., Usuki, T., Lan, C.Y., Chu, H.T., Liou, J.G., 2009. Late Triassic-Late Cretaceous accretion/subduction in the Taiwan region along the eastern margin of South China-evidence from zircon SHRIMP dating. International Geology Review 51, 304-328.

Zelazniewicz, A., Tran, H.T., Larionov, A., 2013. The significance of geological and zircon age data derived from the wall rocks of the Ailaoshan-Red River shear zone, NW Vietnam. J. Geodynamics 69, 122–139.

Zhang, F., Wang, YJ., Chen, X., Fan, W., Zhang, Y., Zhang, G., Zhang, A., 2011. Triassic high-strain shear zones in Hainan Island (South China) and their implications on the amalgamation of the Indochina and south China blocks: kinematics and $^{40}Ar/^{39}Ar$ geochronological constraints. Gondwana Res. 19, 910-925.

Zhao, L., Guo, F., Fan,W.M., Li, C.W., Qin, X.F., Li, H.X., 2012. Origin of the granulite enclaves in Indosinian peraluminous granites, South China and its implication for crustal anatexis. Lithos 150, 209–226.

Zhong, D. 2000, Paleotethysides in West Yunnan and Sichuan, China. Science Press, Beijing, 248pp.

565 Zhou, X.M., Li, W.X. 2000. Origin of Late Mesozoic igneous rocks in Southeastern China:
566 implications for lithosphere subduction and underplating of mafic magmas. Tectonophysics,
567 326, 269-287.
568
569 Zhu, MF., Zhao, JH., Qi, L., Su, W., Hu, R., 2006. Zircon U-Pb geochronology and elemental
570 and Sr-Nd isotope geochemistry of Permian mafic rocks in the Funning area, SW China.
571 Contribution Mineral. Petrol. 151, 1-19.
572
573 Zhu Z., Lao Q., Chen H., Ding S., Liao Z. 1998. Early Mesozoic orogeny in Fujian, Southeast
574 China. Hall R. & Blundell D. (eds) Tectonic Evolution of Southeast Asia. Geol. Soc. Special
575 Pub. 106, 549-556.
576
577 Zi, J.W., Cawood, P., Fan WM., Yang, YJ., Tohver, E., McCuaig, C., Peng, TP. 2012.
578 Triassic collision in the Paleo-Tethys Ocean constrained by volcanic activity in SW China.
579 Lithos 144-145, 145-160.
580
581
582 Figure Captions
583
584 Fig. 1. Schematic map of Central-Eastern Asia showing the main continental blocks,
585 ophiolitic sutures and faults. SCB: South China Block, D: Dabieshan, XFS: Xuefengshan,
586 RRF: Red River Fault, LMS: Longmenshan. Pink lines denote the Triassic belts discussed in
587 this paper. Diamond in Mindoro Island locates the Permian magmatic arc.
588

589 Fig. 2. Tectonic map of the South China Block with emphasis of the Triassic events. The light
590 pink area represents the Xuefengshan belt. RRF: Red River Fault, SCS: Song Chay suture,
591 SMS: Song Ma suture, CLF: Chenzhou-Linwu fault, MXT: Main Xuefeng Thrust, JSF:
592 Jiangshan-Shaoxing fault, DBF: Dien Bien Fu fault. NEV: NE Vietnam belt, DNCV: Day Nui
593 Con Voi Triassic arc, DS: Darongshan pluton, SB: Shiwandashan Mesozoic basin. The cross
594 sections (Fig. 2A, B, C) are located.
595
596 Fig. 3. Crustal scale cross sections of the Triassic belts
597 A: NW Vietnam-S China profile (simplified from Faure et al., 2014). B: Hainan profile. C:
598 Yunkai profile.
599
600 Fig. 4. Field pictures of the Triassic belts. A: Late Triassic red beds unconformably overlying
601 subvertical Middle Triassic turbidite (Jinshajiang, E. of Dexing).
602 B: Bedding (S0) and cleavage (S1) relationships in Middle Triassic limestone indicate a NE-
603 verging fold. A down-dip stretching lineation is observed in the S1 surface (Ailaoshan). C:
604 Permian limestone overthrusting Middle Triassic turbidite (S. Guangxi). D: Early Paleozoic
605 porphyritic granite deformed as orthogneiss with top-to-the-N shearing (Yunkai massif). E:
606 N-verging fold in Devonian sandstone, in the footwall of the Yunkai thrust (Luoding). F:
607 Carboniferous limestone olistolith in a Permian-Triassic siltite matrix (Hainan).
608
609 Fig. 5. Crustal scale cross section of the intracontinental Xuefengshan belt (modified from
610 Chu et al. 2012a). Folding and shearing, pre-dated by the emplacement of Late Triassic
611 plutons accommodated the SE-ward underthrusting of the Western part of the SCB below its
612 Eastern part. S1, S2, S3 are the cleavage planes related to the Triassic deformation phases (cf
613 Chu et al., 2012a for detail).

Fig. 6. Lithosphere scale interpretative cross section from the Xuefengshan to the SE coast of SCB depicting the Triassic deformation. The Early Paleozoic and Cretaceous events have been omitted for clarity. The Triassic geodynamics of the S. part of the SCB are interpreted as the consequence of intracontinental subduction in the Xuefengshan and collision of the SCB with a continental block equivalent to Indochina presently hidden below the S. China Sea. Evidence for a magmatic arc is documented in Hainan Island and in W. Philippines.

Fig. 7. Schematic map showing the main Triassic tectonic features of the South margin of the SCB. At variance with the previous interpretations, this cartoon emphasizes the southward continental subduction of the SCB below the Indochina Block and its eastward extension in W. Philippines that was located South of the SCB before the opening of the South China Sea. Collision was preceded by oceanic subduction that gave rise to several magmatic arcs, namely: W. Ailaoshan, Sam Nua, Dai Nuy Con Voi, Wuzishan, Mindoro. JSJ: Jinshajiang suture, AS: Ailaoshan suture, SMS: Song Ma suture, SCS: Song Chay suture, HS: Hainan suture. Terrigenous deposits of the Shiwandashan basin (SB) unconformably cover the folds and thrusts of the Middle Triassic Youjiang basin. The intracontinental Xuefengshan Belt developed in response to the SE-ward continental subduction of the basement of the SCB. MXT: Main Xuefengshan Thrust. Dotted lines represent the fold axes. The Triassic E-W to NE-SW striking folding developed in the Neoproterozoic Jiuling Massif corresponds to a dextral ramp of the Xuefengshan belt. The Triassic plutons have been omitted for clarity.

Figure 1

Click here to download high resolution image

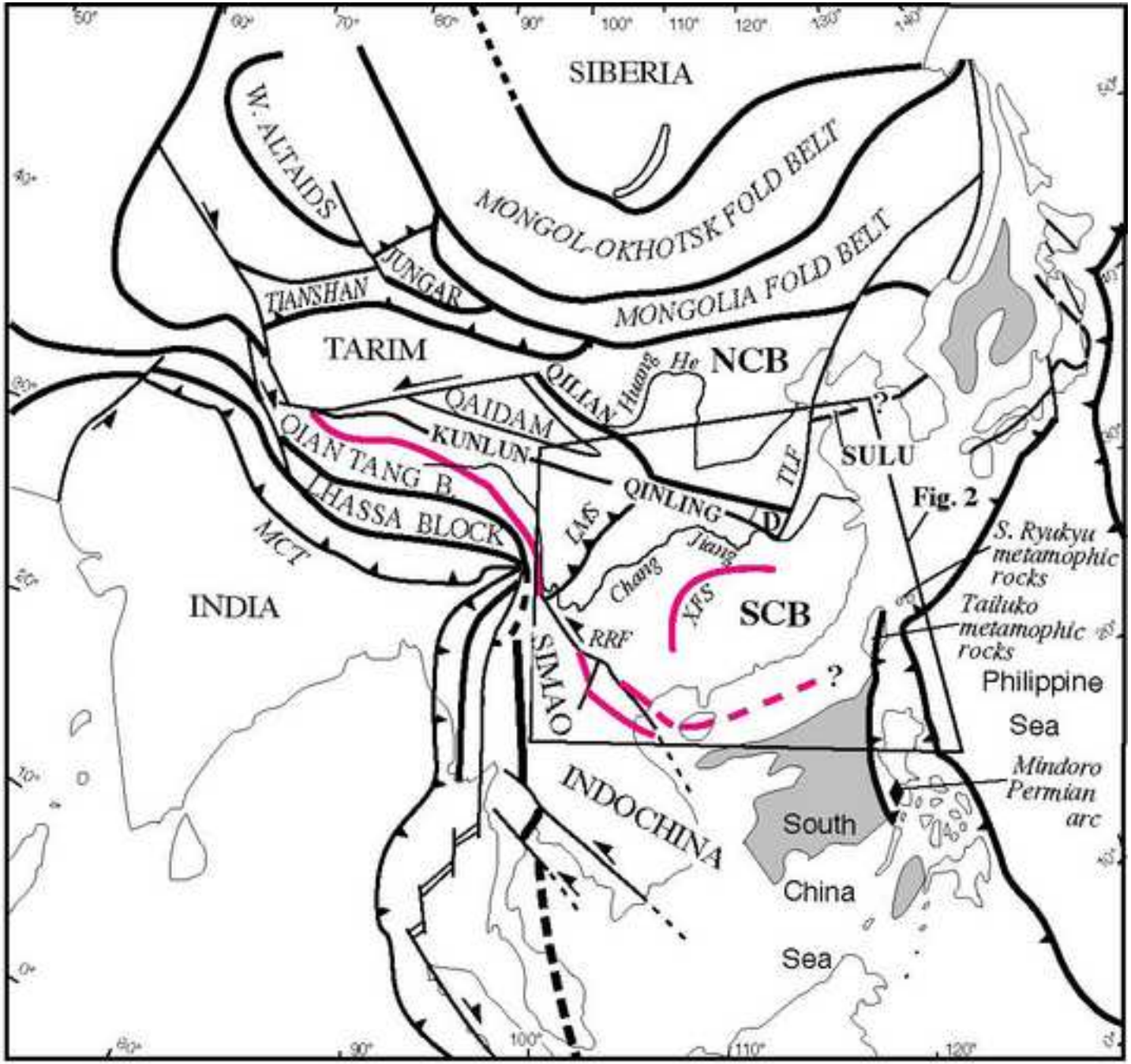

Fig. 1

Figure 2

Click here to download high resolution image

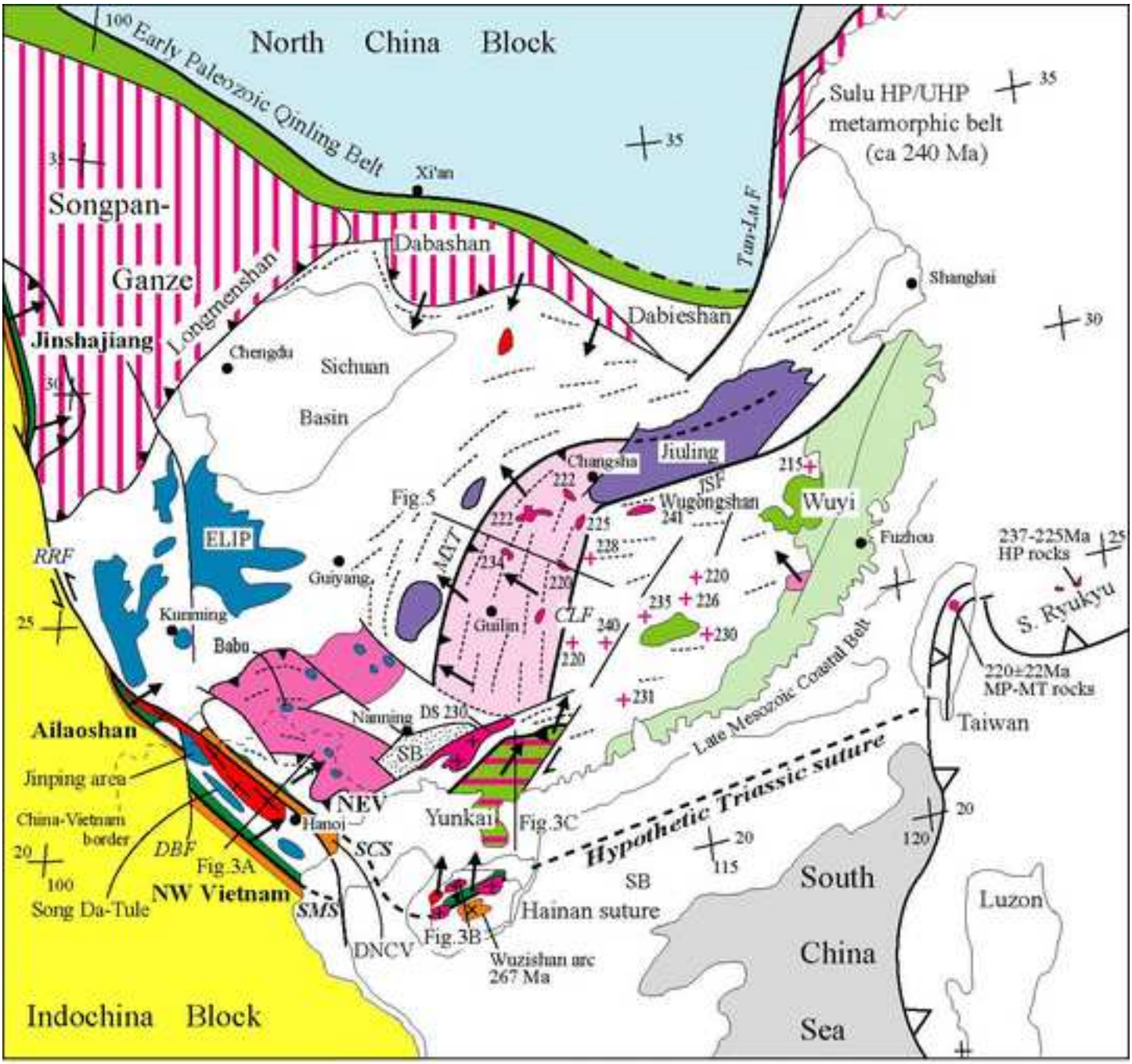

Fig. 2

Figure 3

Click here to download high resolution image

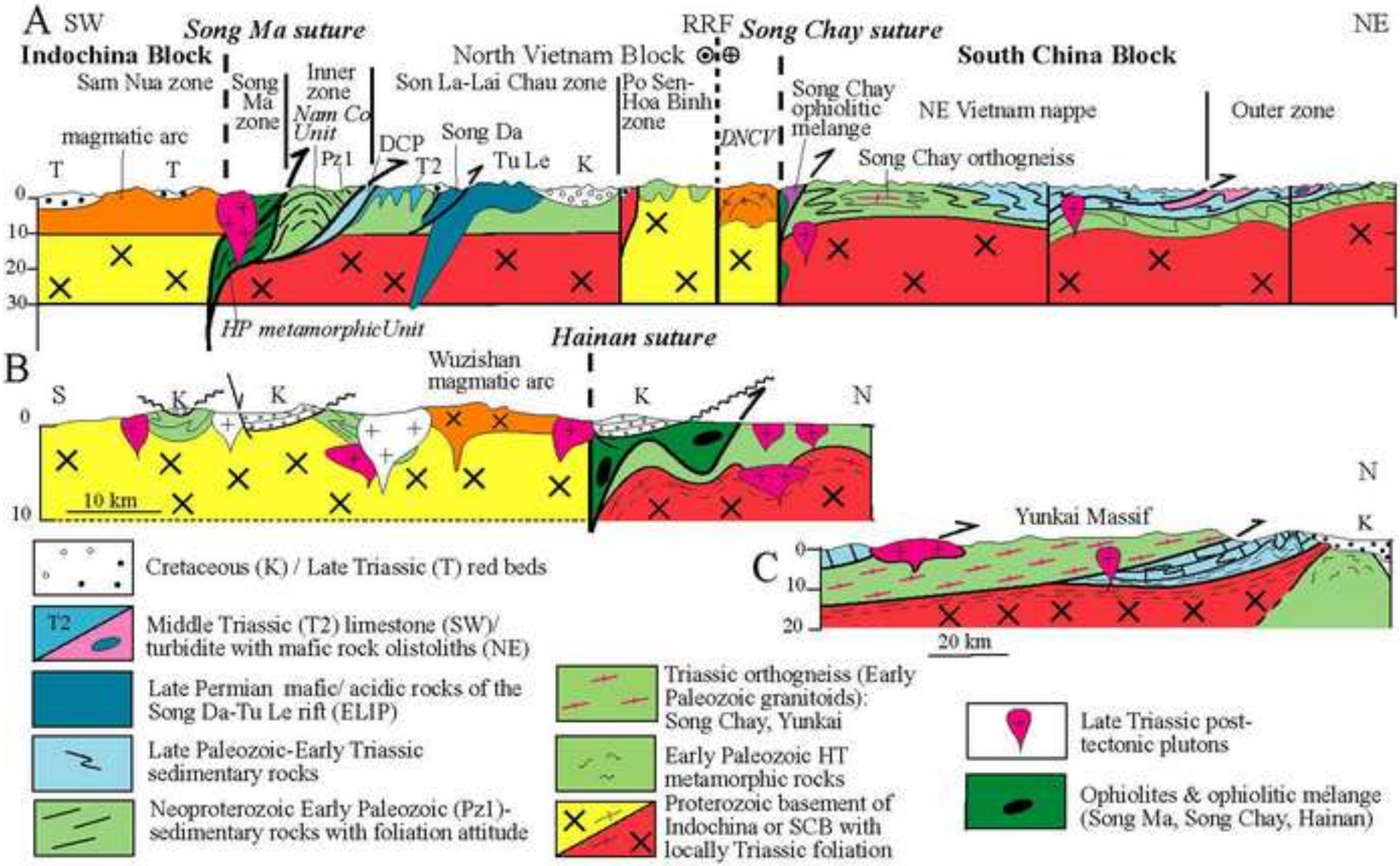

Fig. 3

Figure 4

Click here to download high resolution image

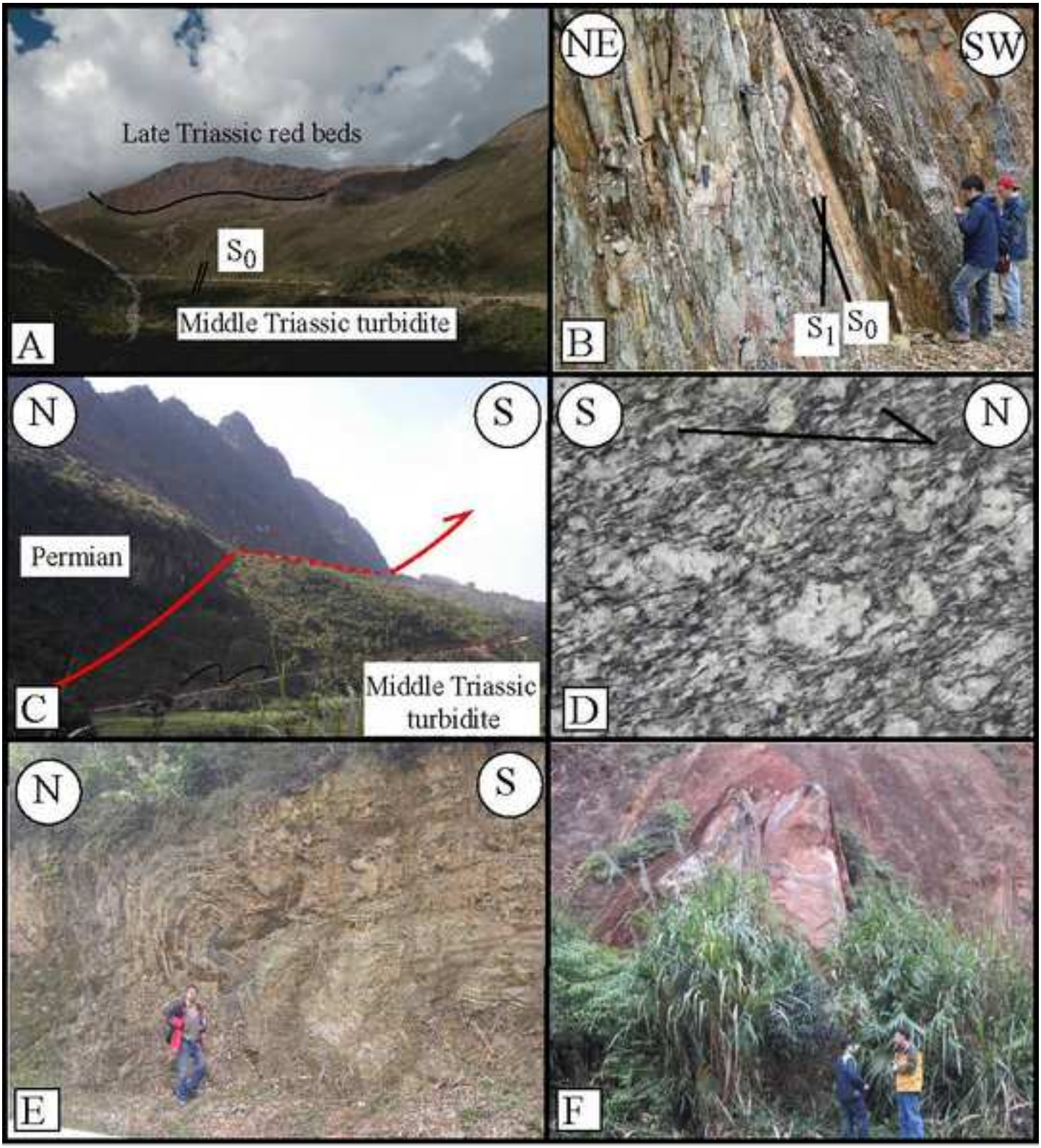

Fig. 4

Figure 5

Click here to download high resolution image

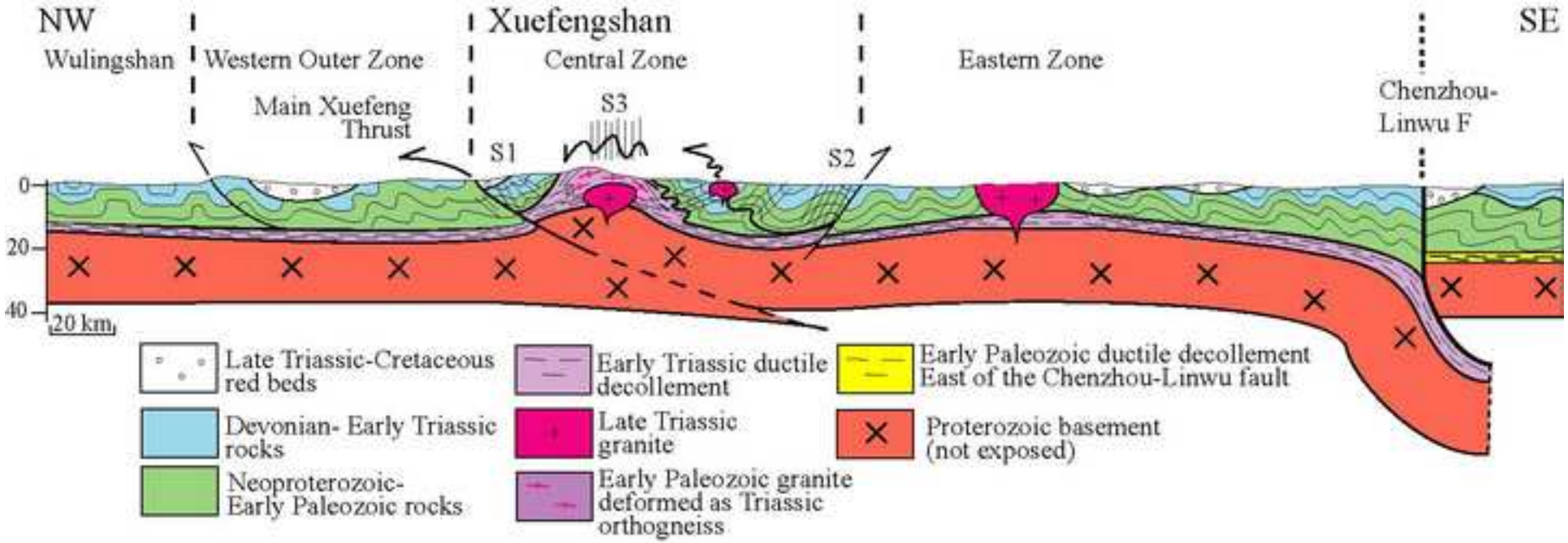

Fig 5

Figure 6

Click here to download high resolution image

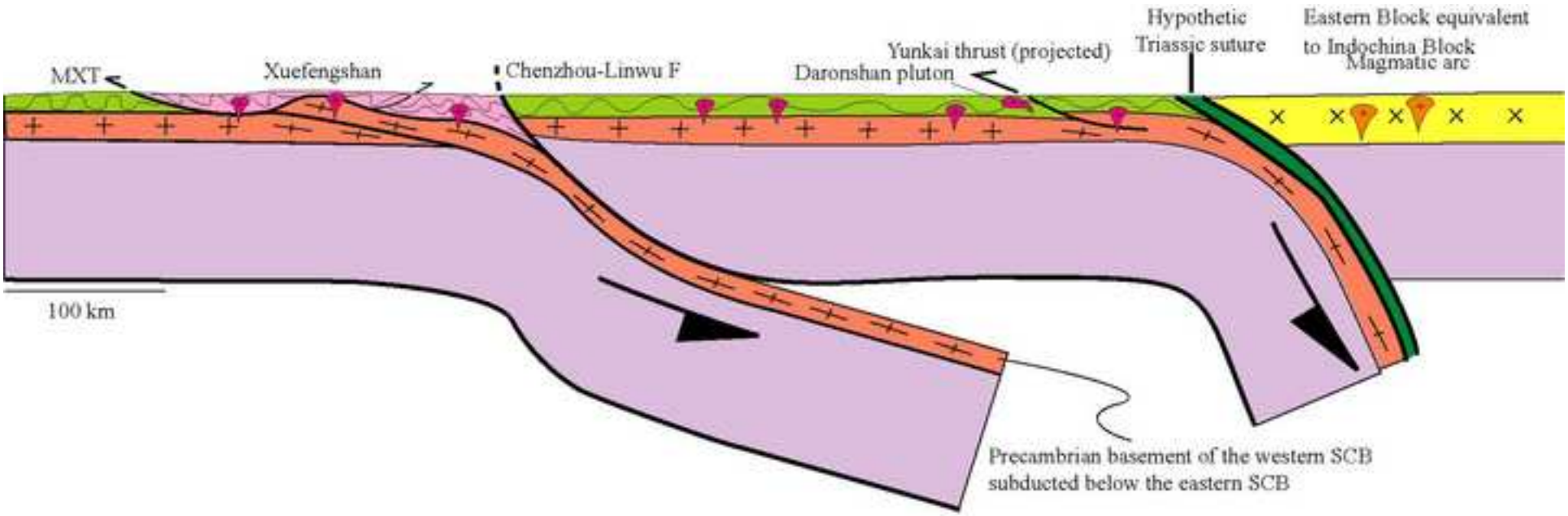

Fig. 6

Figure 7
Click here to download high resolution image

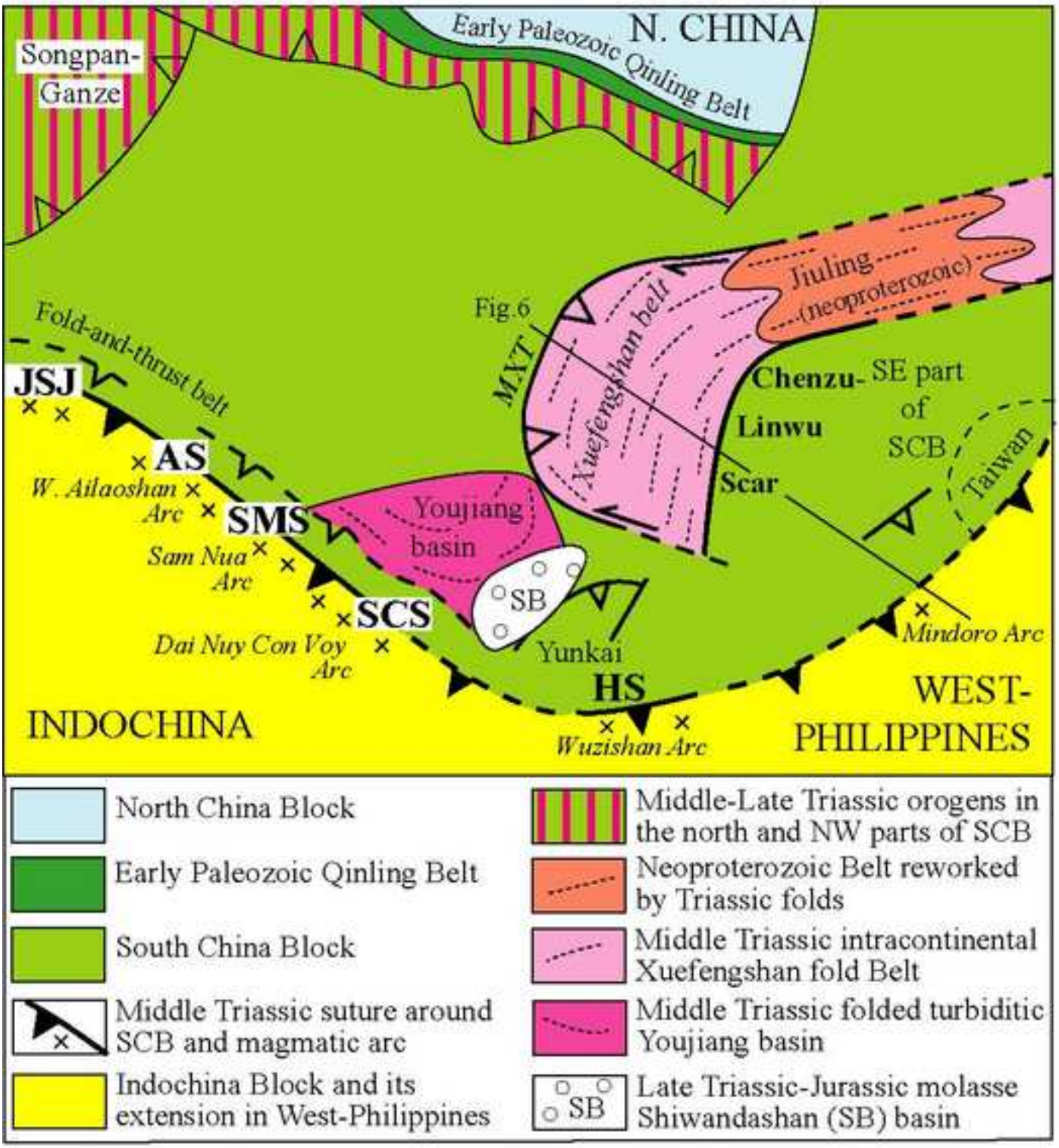

Fig.7